Surface Characteristics of Nanoparticles Determine Their Intracellular Fate in and Processing by Human Blood–Brain Barrier Endothelial Cells *In Vitro*

Julia V Georgieva[1], Dharamdajal Kalicharan[2], Pierre-Olivier Couraud[3,4], Ignacio A Romero[5], Babette Weksler[6], Dick Hoekstra[1] and Inge S Zuhorn[1]

[1]*Section of Membrane Cell Biology, Department of Cell Biology, University Medical Center Groningen, University of Groningen, Groningen, The Netherlands;* [2]*Section of Molecular Imaging and Electron Microscopy, Department of Cell Biology, University Medical Center Groningen, University of Groningen, Groningen, The Netherlands;* [3]*Institut Cochin, Université Paris Descartes, CNRS (UMR 8104), Paris, France;* [4]*Inserm U567, Paris, France;* [5]*Department of Biological Sciences, The Open University, Milton Keynes, UK;* [6]*Department of Medicine, Weill Medical College, New York, New York, USA*

A polarized layer of endothelial cells that comprises the blood–brain barrier (BBB) precludes access of systemically administered medicines to brain tissue. Consequently, there is a need for drug delivery vehicles that mediate transendothelial transport of such medicines. Endothelial cells use a variety of endocytotic pathways for the internalization of exogenous materials, including clathrin-mediated endocytosis, caveolar endocytosis, and macropinocytosis. The different modes of endocytosis result in the delivery of endocytosed material to distinctive intracellular compartments and therewith correlated differential processing. To obtain insight into the properties of drug delivery vehicles that direct their intracellular processing in brain endothelial cells, we investigated the intracellular processing of fixed-size nanoparticles in an *in vitro* BBB model as a function of distinct nanoparticle surface modifications. Caveolar endocytosis, adsorptive-mediated endocytosis, and receptor-mediated endocytosis were promoted by the use of uncoated 500-nm particles, attachment of the cationic polymer polyethyleneimine (PEI), and attachment of prion proteins, respectively. We demonstrate that surface modifications of nanoparticles, including charge and protein ligands, affect their mode of internalization by brain endothelial cells and thereby their subcellular fate and transcytotic potential.

Received 2 March 2010; accepted 4 October 2010; published online 2 November 2010. doi:10.1038/mt.2010.236

INTRODUCTION

The effectiveness of therapeutic compounds is often limited by the fact that following their systemic administration they do not reach their target site. This holds, in particular, for treatment of brain-related diseases where drugs fail to reach their target site, *i.e.* the brain, because brain tissue is protected from the systemic circulation by the blood–brain barrier (BBB). The BBB is composed of a layer of tightly connected endothelial cells, supported by astrocytic end feet. Transport across the BBB is restricted to small lipophilic compounds and nutrients that are carried by specialized transporters. In addition to membrane passage mediated by such specific transporters, endothelial cells, whose membrane surface is polarized, exploit the process of transcytosis, *i.e.* endocytosis at the apical (blood) side of the endothelium followed by exocytosis at the basolateral (tissue) side, to deliver nutrients, such as cholesterol and iron, to the underlying tissue. Although the application of nanoparticles for drug delivery could greatly extend the variety of drugs that could potentially be translocated across the BBB, a relevant issue to their rational design is how a cell distinguishes cargo from simple endocytotic internalization for its own use, as compared to transcytosis for use by the underlying tissue. The molecular mechanisms that underlie entry into either of these pathways are largely unknown. It is reasonable to suggest that the entry pathway itself is a decisive factor in diverting cargo/receptor-dependent subcellular trafficking and thereby the cargo's fate. Support comes from a study on chimeric AB5 toxins in which the binding of the toxin to GD1a instead of its natural receptor GM1 was shown to preclude its uptake *via* caveolae, while the GD1a-mediated pathway resulted in inactivity of the toxin.[1] However, the association of receptors with certain entry modalities may vary between cell types and species.

Transcytosis of macromolecules in endothelial cells is most likely mediated by caveolae or caveolae-like membrane domains, *i.e.* rafts.[2–5] Inducing the uptake of nanoparticles *via* raft-dependent endocytosis may therefore possibly lead to their transcytosis. In addition, a cationic charge on the (macro) molecules promotes their electrostatic interaction with the negatively charged cell surface, leading to an enhanced cellular uptake *via* adsorptive endocytosis, which seems to be receptor independent. In brain vascular endothelial cells, evidence for a tight correlation between the process of adsorptive endocytosis and transcytosis has been demonstrated. Indeed, the covalent linkage of primary amine

Correspondence: *Inge S Zuhorn, Department of Cell Biology, Section of Membrane Cell Biology, University Medical Center Groningen, University of Groningen, A. Deusinglaan 1, Groningen 9713 AV, The Netherlands. E-mail: i.zuhorn@med.umcg.nl*

groups to the surface of IgG molecules, thereby conveying cationic charge, has been shown to promote delivery across the BBB *via* adsorptive-mediated transcytosis.[6] Likewise, cationization of albumin also increases its transport across the BBB.[7] Finally, ligands of BBB receptors, showing a transcytotic capacity, have been described, including low-density lipoprotein[8] and transferrin,[9,10] and molecules that bind to these receptors may serve as drug delivery vehicles.[11–13]

The aim of this study was to determine whether surface modifications of a nanoparticle of a fixed size can target the nanoparticle to a specific endocytotic pathway in human brain endothelial cells, *i.e.*, caveolar endocytosis, adsorptive-mediated endocytosis, or receptor-mediated endocytosis, which may allow subsequent transcytosis. Large size (*i.e.* 500 nm) nanoparticles were used for targeting to a caveolae-mediated entry route, based on previous observations that latex particles with a diameter ≥500 nm are internalized by nonphagocytic B16 cells through caveolae, whereas particles up to 200 nm in diameter are efficiently taken up *via* clathrin-mediated endocytosis.[14] Nanoparticles carrying a net cationic charge, accomplished by nanoparticle surface modification with polyethyleneimine (PEI) were made for targeting to an adsorptive endocytotic route. Finally, to target nanoparticles of 500 nm into a receptor-mediated endocytotic route, the nanoparticles were decorated with a ligand, *i.e.*, prion protein to induce binding to a receptor, known to mediate transcytosis from the apical surface of brain endothelial cells.[15,16] Our data reveal that specific surface modification of a nanoparticle of a given size modifies its entry pathway and processing in human BBB endothelial hCMEC/D3 cells, and thereby the transendothelial transport potential.

RESULTS

Nanoparticles with distinct surface modifications interact differently with the surface of human brain endothelial cells

It is plausible that nanoparticles with modified surface characteristics interact differently with the cell surface. Therefore, we investigated the interaction of the different surface-modified nanoparticles with the plasma membrane of human BBB endothelial hCMEC/D3 cells at the ultrastructural level by transmission electron microscopy. Noncoated beads (NBs) were predominantly observed near electron-dense regions of the plasma membrane (**Figure 1a**, arrowheads). In addition, NBs were frequently found to be surrounded by smooth plasma membrane protrusions (**Figure 1b**). Most PEI-coated beads (PEIBs) were also found to be engulfed by plasma membrane protrusions (**Figure 1d**). However, in striking contrast to the smooth protrusions surrounding NBs (**Figure 1b**), plasma membrane surrounding PEIBs typically contained electron-dense regions (**Figure 1d**, arrowheads). In contrast to NBs and PEIBs, engulfment of prion-coated beads (PrPBs) was never observed. Instead, PrPBs were primarily observed at surface domains marked by a relatively thin electron-dense coat (**Figure 1c**, arrows, compare to **Figure 1a**), which showed only minor indentation. These data demonstrate that surface modification of 500-nm beads influences their interaction with the plasma membrane of hCMEC/D3 cells. Because electron-dense plasma membrane regions and protrusions are typically involved

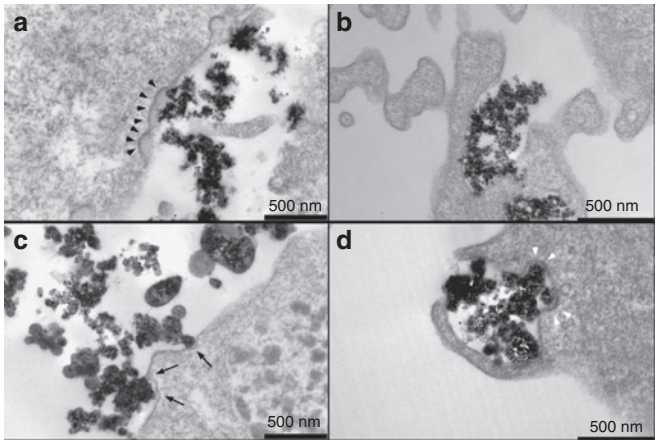

Figure 1 Uptake of nanoparticles by hCMEC/D3 cells. hCMEC/D3 cells were incubated with NBs, PrPBs, and PEIBs, and investigated with electron microscopy. (**a**) NBs are found interacting with electron-dense plasma membrane (arrowheads) or (**b**) within cellular extensions. (**c**) PrPBs show binding to less pronounced electron-dense regions at the plasma membrane (arrows). (**d**) Cellular protrusions embrace PEIBs. Structures resembling clathrin-coated pits are indicated with white arrowheads. NB, noncoated bead; PEIB, polyethyleneimine-coated bead; PrPB, prion-coated bead.

in (distinct routes of) internalization,[17–19] we next investigated the effect of metabolic inhibitors of endocytosis on the uptake of the different surface-modified particles.

Nanoparticles with distinct surface modifications respond differentially to metabolic inhibitors of distinct endocytotic pathways

To obtain support that NBs, PrPBs, and PEIBs are internalized *via* distinct endocytotic pathways, we investigated their response to a variety of metabolic inhibitors that are well-known to preferentially perturb clathrin-mediated endocytsosis, raft/caveolae-mediated endocytosis, and macropinocytosis. Polarized hCMEC/D3 cells (**Supplementary Figure S1**) were treated with filipin III (1 µg/ml), okadaic acid (150 mmol/l), genistein (30 µg/ml), dimethylamiloride (40 µmol/l), chlorpromazine (5 µg/ml) at 37 °C for 30 minutes. Filipin III, okadaic acid, and genistein have been reported to inhibit raft/caveolae-mediated endocytosis, while minimally affecting clathrin-mediated endocytosis or macropinocytosis.[20–22] Importantly, we confirmed that also in hCMEC/D3 cells these compounds significantly inhibited the uptake of fluorescein isothiocyanate–labeled cholera toxin B, a marker for raft/caveolae-mediated endocytosis,[23] whereas the uptake of transferrin (marker for clathrin-mediated endocytosis[24]) and fluorescein isothiocyanate–labeled dextran (marker for macropinocytosis[25]) was not affected (**Supplementary Table S1**). Chlorpromazine and dimethylamiloride are well known for their inhibitory effect on clathrin-mediated endocytosis and macropinocytosis, respectively.[26] Indeed, also in hCMEC/D3 cells, the uptake of transferrin and fluorescein isothiocyanate–dextran was preferentially inhibited by chlorpromazine and dimethylamiloride. In agreement with reports in other cell types, the uptake of fluorescein isothiocyanate–dextran in hCMEC/D3 cells was most dramatically inhibited by dimethylamiloride (**Supplementary Table S1**).

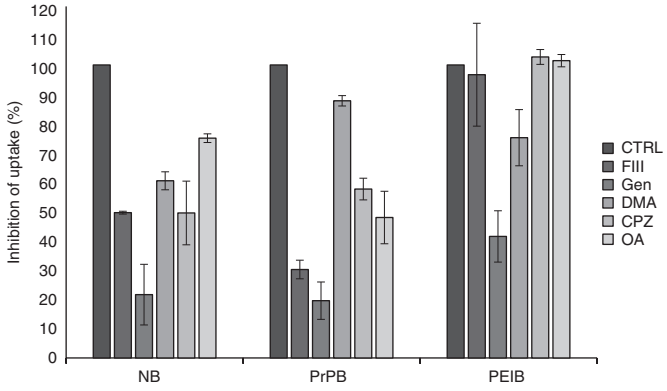

Figure 2 Effect of metabolic inhibitors of endocytosis on the uptake of nanoparticles. hCMEC/D3 cells were treated with filipin III (FIII; 1 µg/ml), genistein (Gen; 30 µg/ml), dimethylamiloride (DMA; 40 µmol/l), chlorpromazine (CPZ; 5 µg/ml), and okadaic acid (OA; 150 nmol/l) for 30 minutes. Nanoparticles were added and incubated for 1 hour 30 minutes. After extensive washing, the cells were fixed and analyzed with confocal microscopy. Five randomly selected fields of each experimental condition of two independent experiments were scanned and the number of detected nanoparticles was quantified with ImageJ (National Institutes of Health). Results are presented as percentage of the total input (mean±SEM, n = 2). CTRL, control; NB, noncoated bead; PEIB, polyethyleneimine-coated bead; PrPB, prion-coated bead.

Having confirmed the differential inhibition of distinct endocytotic pathways by these compounds in hCMEC/D3 cells, we next incubated the pretreated cells with NBs, PrPBs, or PEIBs at 37 °C for 90 minutes, which allows for the endocytosis of a significant fraction of applied nanoparticles. Noninternalized nanoparticles were washed, cells were fixed, and internalization of the nanoparticles was determined as described in Materials and Methods. As shown in **Figure 2**, the internalization of NBs was most effectively inhibited (78.3±10.3%) by genistein. In addition, fillipin III, okadaic acid, chlorpromazine, and dimethylamiloride in part inhibited the uptake of NBs with 50.5±0.4, 25±1.4, 50.5±10.8, and 39.5±3%, respectively. These data suggest that NBs may be internalized *via* multiple endocytotic pathways, but with a preference for a genistein-sensitive pathway. The uptake of PrPBs was highly sensitive to treatment with fillipin III, genistein, and okadaic acid (79.8±3.1, 80.4±6.3, and 52.1±8.9% inhibition, respectively). In addition, uptake of PrPBs was partly inhibited by chlorpromazine (42.4±3.7%) and minimally inhibited by dimethylamiloride (12.3±1.7%). These data suggest that the uptake of PrPBs is primarily sensitive to inhibitors of caveolae/raft-mediated endocytosis. The uptake of PEIBs was inhibited by genistein (68.6 ± 8.7%) and dimethylamiloride (24.9±9.5%), whereas fillipin III, okadaic acid, and chlorpromazine were without effect. Taken together, these data clearly demonstrate that the uptake of NBs, PrPBs, and PEIBs is differentially inhibited by these compounds, and therefore suggest that NBs, PrPBs, and PEIBs are endocytosed *via* distinct pathways.

Endocytosed nanoparticles with distinct surface modifications move through different endocytotic compartments in brain endothelial cells

In order to further investigate the endocytotic pathway and fate of NBs, PrPBs, and PEIBs, we determined their colocalization with proteins known to mark distinct endocytotic pathways and/or compartments as a function of time (**Figure 3**). First, we determined colocalization of the particles with rabankyrin-5, a rab5-effector that has been implicated to play a role in macropinocytosis.[27] Following an incubation at 37 °C for 30 minutes, very little (<3%) colocalization between NBs or PrPBs with rabankyrin-5 was found whereas, by contrast, ~43.6±17% of the PEIBs were found to colocalize with rabankyrin-5 (**Figure 3a**). NBs also did not significantly (4.8±8.3%) colocalize with early endosomal antigen (EEA)-1, a protein that marks early sorting endosomes. In contrast, PrPBs and PEIBs did show significant colocalization with EEA-1 (33.6±2.4 and 55.1±15.4%, respectively, **Figure 3b**). Both NBs and PrPBs colocalized with caveolin-1 (23.7±0.3 and 18.6±1.48%, respectively) but not with clathrin (<5%) after a 30-minute incubation. In contrast, PEIBs showed only little (5.7±1.7%) colocalization with caveolin (**Figure 3c**), but substantially colocalized with clathrin (49.8±5.3%). After a 60-minute incubation, NBs and PrPBs still colocalized with caveolin-1 (24.7±4.9 and 16.8±0.8%, respectively) and negligible colocalization with clathrin was observed (**Figure 3d**). PEIBs showed little (5.3±1.6%) colocalization with caveolin-1 but extensively colocalized with clathrin (45.5±5.7%). At this time point, colocalization with rab11a (**Figure 3e**), a marker of recycling endosomes, was observed for PEIBs (29.6±11.1%), but not NBs (1.8±2.6%) and PrPBs (0%). After a 90-minute incubation, the colocalization of NBs with caveolin-1 decreased to <5% (**Figure 3f**). By contrast, PrPBs showed an increasing colocalization with both caveolin-1 (47.8±6.1%) and clathrin (25.6±1%). PEIBs showed little (<5%) colocalization with caveolin-1 but extensively colocalized with clathrin (58.1±3.6%), similar to that observed after 30- and 60-minute incubation. After a prolonged, 18-hour incubation, 24.9±6.3 and 14.3±4.5% of the NB and PEIBs, respectively, colocalized with Lamp-1 (**Figure 3g**) and lysotracker (data not shown), which are markers of the more acidic late endosomes and lysosomes. In contrast, only 5.5±1.5% of PrPBs colocalized with Lamp-1 at this time point. In summary, NBs followed an endocytotic pathway that is, in part, transiently marked by the presence of caveolin-1, but not clathrin, EEA-1 or rabankyrin-5, and led to late endosomes and/or lysosomes. PrPBs followed an endocytotic pathway that is in part marked by EEA-1 and increasingly marked by caveolin-1, but not clathrin or rabankyrin-5, and avoided late endosomes and/or lysosomes. PEIBs followed an endocytotic pathway that is substantially marked by rabankyrin-5, EEA-1, and rab11a, but to a much lesser extent caveolin-1 and, in part, led to late endosomes and/or lysosomes. These data clearly demonstrate that human endothelial cells differentially internalize and process NBs, PrPBs, and PEIBs.

Endocytosed nanoparticles with different surface modifications are delivered to morphologically distinct intracellular compartments in brain endothelial cells

We next examined the identity of the intracellular compartment to which the particles were delivered following 90-minutes incubation at the ultrastructural level by transmission electron microscopy (**Figure 4**). NBs were detected in large vacuoles containing numerous small (50–100 nm diameter) internal vesicles,

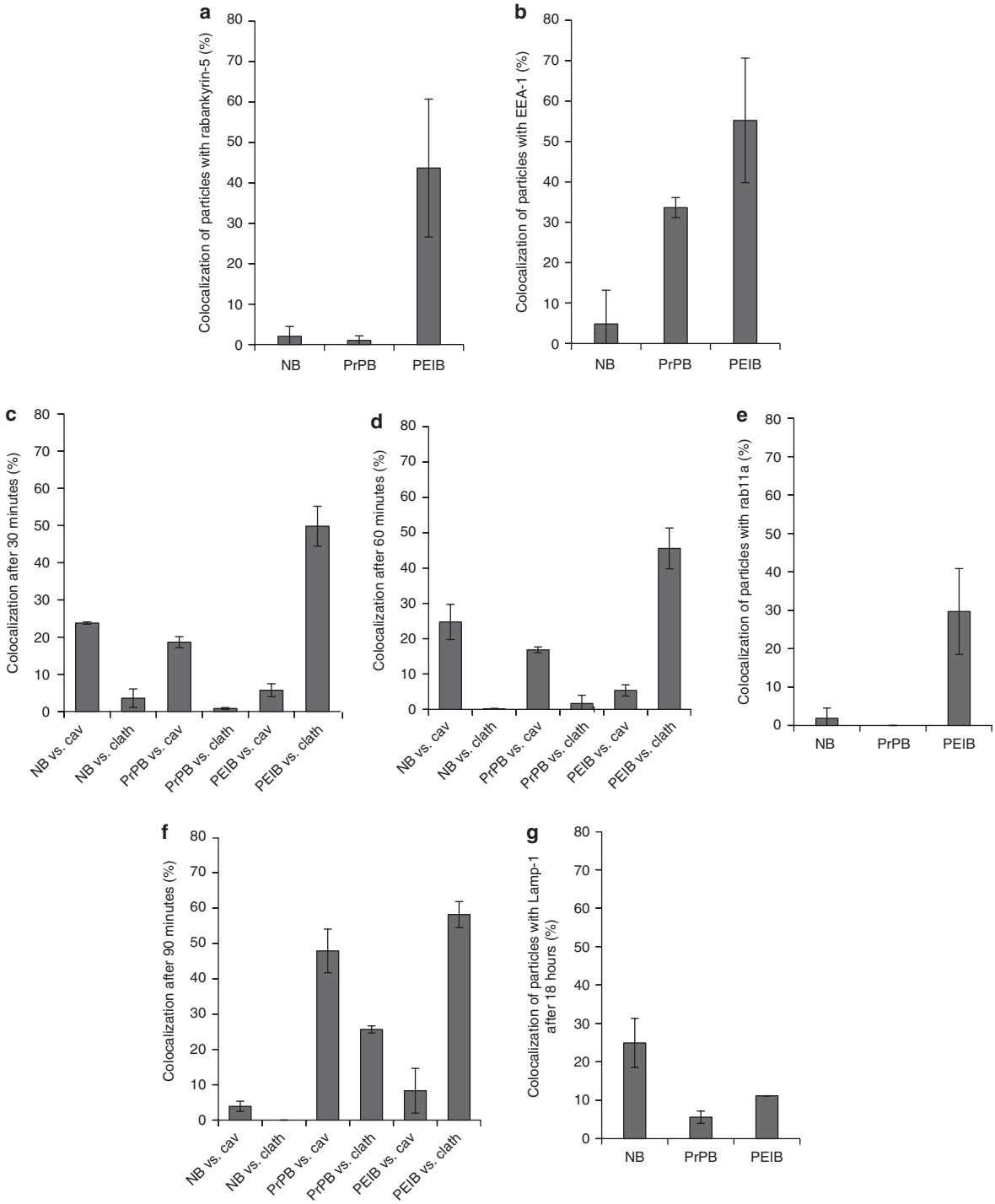

Figure 3 Colocalization of nanoparticles with rabankyrin-5, EEA-1, caveolin-1, clathrin, rab11, and Lamp-1. hCMEC/D3 endothelial cells were incubated with nanoparticles for 30 minutes at 4 °C. Subsequently, cells were incubated for (**a–c**) 30 minutes, (**d**,**e**) 60 minutes, (**f**) 90 minutes, and (**g**) 18 hours at 37 °C to allow particle internalization. (**a**) NBs and PrPBs do not colocalize with rabankyrin-5. A significant fraction of PEIBs is located in rabankyrin-5-positive vesicles. (**b**) NBs do not show significant colocalization with the early endosomal marker EEA-1, while 33% of the PrPBs show colocalization with EEA-1. Fifty-five percent of the PEIBs colocalize with EEA-1. (**c**) NBs and PrPBs show a similar extent of colocalization with caveolin-1, around 20%, and clathrin, <5%. In contrast, PEIBs colocalize extensively with clathrin. (**d**) The profile of colocalization of nanoparticles with the markers caveolin and clathrin at 60 minutes is comparable to that at earlier time points. (**e**) NBs and PrPBs lack rab11-colocalization. Around 30% of PEIBs reach a rab11-positive compartment after 60 minutes of internalization. (**f**) NBs are not identified within caveolin- or clathrin-positive compartments. PrPBs show an increase in colocalization with caveolin and clathrin in time. PEIBs continually colocalize with clathrin. (**g**) After 18 hours of incubation of hCMEC/D3 cells with nanoparticles, NBs and PEIBs sporadically colocalize with Lamp-1, whereas PrPBs are not detected in Lamp-1-positives vesicles. Cav, caveolin; clath, clathrin; EEA-1, early endosomal antigen-1; NB, noncoated bead; PEIB, polyethyleneimine-coated bead; PrPB, prion-coated bead.

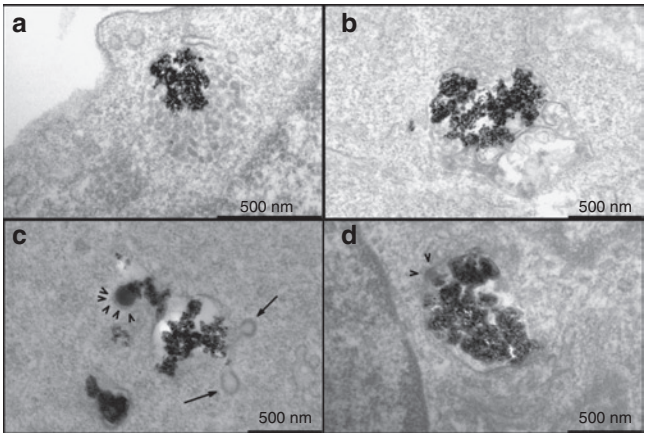

Figure 4 NBs, PrPBs, and PEIBs localize in morphologically distinct intracellular vesicles. hCMEC/D3 cells were incubated with nanoparticles for 1 hour and 30 minutes. (**a**,**b**) NBs were found in vacuoles resembling multivesicular bodies (MVBs) and in multilamellar bodies. (**c**) PrPBs were primarily localized within vesicular structures. Note the presence of clathrin-coated buds (arrows) and the formation of clathrin latices around the prion coat (arrowheads). (**d**) PEIBs resided in large endosomes. Clathrin latices were found around the PEI coat (arrowheads). Bar = 500 nm. NB, noncoated bead; PEIB, polyethyleneimine-coated bead; PrPB, prion-coated bead.

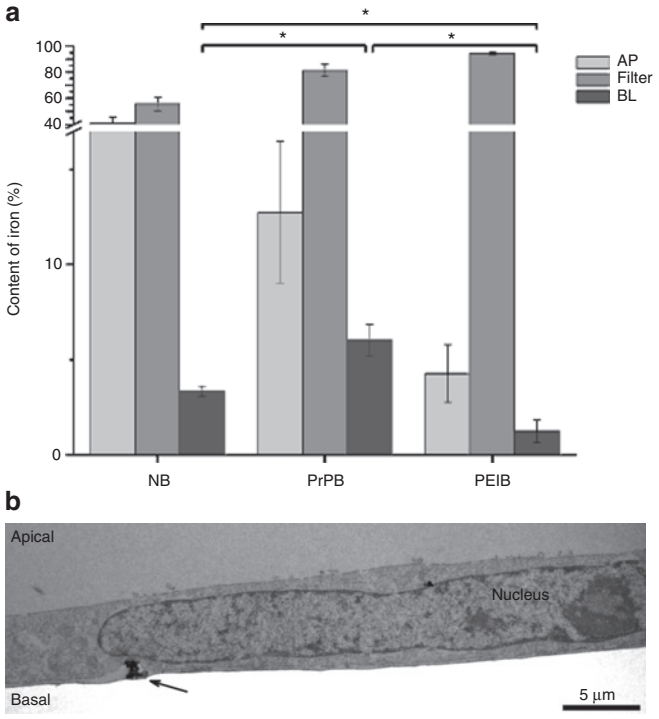

Figure 5 Transcytosis of nanoparticles across a monolayer of endothelial cells. (**a**) hCMEC/D3 cells were cultured on Transwell filters. Nanoparticles were added to the apical compartment and incubated for 18 hours. The total amount of iron was measured in the apical and basal compartment, and in the filter membrane with the cells. Transcytosis is presented as amount of iron in the apical compartment divided by the total amount of iron in the three compartments, and expressed as percentage (mean±SEM, n = 3). Asterisks indicate significant differences ($P < 0.05$) in transcytosis of NBs versus PrPBs, PrPBs versus PEIBs, and NBs versus PEIBs, as evaluated with the Student's t-test. (**b**) Electron micrograph of a prion-coated particle (arrow) exocytosed at the abluminal side of a monolayer of hCMEC/D3 cells. AP, apical; BL, basal; NB, noncoated bead; PEIB, polyethyleneimine-coated bead; PrPB, prion-coated bead.

resembling multivesicular bodies (MVBs; Figure 4a). In addition, NBs were found in multilamellar bodies (Figure 4b). MVBs are typically associated with the degradative pathway. In contrast to NBs, PrPBs were exclusively detected in large vesicular structures that contained multiple electron-dense buds (Figure 4c), reminiscent of clathrin buds. Indeed, ultrastructural analysis by immunoelectron microscopy demonstrated that the PrPBs-containing structures were positive for clathrin, as well as caveolin-1 (**Supplementary Figure S2**), which is consistent with the immunofluorescence confocal laser scanning microscopy data (Figure 3f). The combined presence of caveolin-1 and clathrin is suggestive for a localization of the PrPB in early/sorting endosomes. Of interest, PrPBs were occasionally observed in these coated buds (Figure 4c, arrowheads). PEIBs were found mainly in large vacuoles (Figure 4d) and an electron-dense region was occasionally observed near the entrapped particles. Given the extensive colocalization of PEIBs with clathrin (Figure 3f), these electron-dense regions likely represent clathrin-coated domains. The observed localization of NBs, PrPBs, and PEIBs in intracellular compartments with distinct ultrastructural characteristics, in agreement with the colocalization experiments (Figure 3c,d,f), indicates that surface properties of nanoparticles critically affect their mode of endocytosis and processing by hCMEC/D3 cells.

NBs and PrPBs but not PEIBs show transcytotic potential in brain endothelial cell monolayers

As the endocytotic pathways that were under investigation in this study, *i.e.* raft/caveolar endocytosis, adsorptive-mediated endocytosis, and receptor-mediated endocytosis have all been implicated in mediating transcytosis across the BBB, we next examined the transcytotic potential of NBs, PrPBs, and PEIBs. Nanoparticles were added at the apical side (facing the blood *in vivo*) of a polarized confluent monolayer of hCMEC/D3 cells, grown on Transwell filters. After an 18-hour incubation, the content of the particles in the apical and basolateral compartments as well as the fraction associated with the filter (cells) was quantified. After the indicated time interval of 18 hours, ~94.5±1.0% of the PEIBs, 81.2±4.6% of PrPBs, and 55.7±5.2% of NBs still associated with the endothelial cells (Figure 5a). The capacities of translocation of the nanoparticles across the endothelial monolayer, as reflected by the fraction of apically applied nanoparticles recovered in the basolateral compartment, were 6.0±0.9% for PrPBs, 3.4±0.3% for NBs, and 1.3±0.6% for PEIBs (Figure 5a). The process of exocytosis and release of a prion-coated particle at the abluminal site of an hCMEC/D3 monolayer was confirmed by electron microscopic examination (Figure 5b).

DISCUSSION

In this study, we demonstrate that the coupling of a ligand (prion) or charge (PEI) at the surface of a nanoparticle of a given size modifies its entry pathway and processing in human BBB endothelial hCMEC/D3 cells. Careful analyses suggest that uncoated nanoparticles do not enter in an all-or-nothing or exclusive pathway but following surface modification show preference for a specific pathway(s). As a consequence NBs, PrPBs, and PEIBs are delivered to intracellular compartments that are distinct with regard

to their ultrastructural morphology and composition, *i.e.* MVBs, sorting endosomes, and vacuoles, respectively. The endocytotic pathway of noncoated particles shares characteristics of raft/caveolae-mediated endocytosis and macropinocytosis. The presence of NBs in two distinctive populations of intracellular vesicles, *i.e.* vesicles resembling MVBs and multilamellar bodies, possibly reflects the existence of the two different entry mechanisms. Interestingly, in brain endothelial cells a subcompartment has been characterized that originates from caveolae and morphologically resembles MVBs.[8] This compartment is Lamp-1 positive, but devoid of a degradative function and it is involved in the transcytosis of low-density lipoprotein. In our study, NBs may similarly be internalized *via* rafts/caveolae, and transported to MVBs (**Figure 4a,b**) that are Lamp-1-positive (**Figure 3g**). Whether or not the NB-containing vesicles mature to lysosomes is not known. It should be noted that we never observed electron-dense staining of these (pre)lysosomal structures, indicating the absence of degradative enzymes. The engulfment of PEIBs by plasma membrane protrusions containing clathrin coats, their genistein- and dimethylamiloride-sensitive internalization and colocalization with clathrin and rabankyrin-5 are typical characteristics of macropinocytosis. Notably, the cellular processing of PEIBs lacked characteristics of raft/caveolae-mediated endocytosis, *e.g.* sensitivity to filipin III and okadaic acid and colocalization with caveolin-1. Therefore, the addition of PEI (charge) to the particles appears to stimulate their targeting into a macropinocytotic entry pathway, leading to distinctive and large intracellular vacuoles. The surface modification of the particles with prion protein resulted in a clear difference in the way these particles (PrPBs) are processed by hCMEC/D3 cells when compared to NBs and PEIBs. PrPBs were found in compartments that displayed characteristics of early/sorting endosomes (**Figure 4c**), compartments that were positive for both caveolin-1 and clathrin (**Figure 3f**). In addition to binding cholesterol and inhibiting caveolar endocytosis, filipin has been described to cause the release of prion protein from the plasma membrane and reduce the endocytosis of prion protein,[28] which may explain its strong effect on the internalization of PrPBs, when assuming a homophilic interaction between the PrPBs and native prion present on the hCMEC/D3 cells.

Our data underscore that varying the surface properties of nanoparticles results in significant changes in their uptake mechanism, and consequently, their processing by the cells. Clearly, by surface modification of nanoparticles, subcellular targeting into endocytotic pathways and cellular organelles of choice can be achieved. The physicochemical characteristics of (nano)particles, including size, and surface characteristics (charge and/or presence of ligands), are important parameters that dictate their cellular processing. The relevance of the physicochemical properties of nanoparticles for determining the intracellular trafficking is an important and emerging theme in the field of drug delivery.[29] With respect to delivery to brain tissue, it will be of particular interest to further identify physicochemical properties of nanoparticles that preferentially result in particle transcytosis.

Transcytosis of drugs and/or their transport vehicles by vascular endothelial cells is thought to be instrumental in accomplishing transport across the BBB for drug delivery into brain tissue. In this work, we determined the transcytotic capacity of human brain endothelial cells (hCMEC/D3), as an *in vitro* model for the BBB. Our data show that PEI coating of the nanoparticles inhibits their transcytotic potential when compared to noncoated nanoparticles. By contrast, our data show that coating of the nanoparticles with prion improves transcytosis in comparison to NBs and PEIBs, which is consistent with a relatively enhanced transport of these targeted nanoparticles across the endothelial barrier as visualized by nanoparticle delivery into the basolateral compartment in Transwell grown cell cultures. Prion is best known for the capacity of its infectious scrapie isoform to invade an organism after oral ingestion, leading to degenerative and fatal neurological disorders belonging to the group of transmissible spongiform encephalopathies. Following oral administration, prion crosses the intestinal epithelial barrier *via* transcytosis. Subsequently, prion may infect monocytes and/or is transported along nerves in a retrograde fashion and reaches the brain.[30,31] Recently, it was shown that scrapie prion as well as the cellular prion are able to translocate across the BBB, from blood into brain,[16,32] which represents an alternative pathway for infection. Although being differently processed by cultured hCMEC/D3 cells, the PrPBs and NBs both showed transcytotic activity. However, *in vivo* prion may serve a dual role: first, to target nanoparticles in the blood stream to the brain, and second to initiate their transcytosis.

Although the transcytotic efficiency of the nanoparticles reported in this study remains limited, it is in the range of transcytosis across endothelial cells that is typically achieved with exogenous materials. Transcytosis of human immunodeficiency virus-1 viral particles across brain microvascular endothelial cells was shown to be 1% of the added dose after a 24-hour incubation period,[26] while the level of transcytosis for adenovirus-5 viral particles in brain microvascular endothelial cells was 0.1% (6 hours).[33] Redirection of adenovirus-5 into the melanotransferrin (MTf/p97) transcytotic pathway by surface modification of the viral particles with melanotransferrin resulted in transport of 5% of viral particles across the BBB.[33] In future work, the influence of inflammatory signals and signals secreted by (cholesterol-depleted) astrocytes, which have been reported to modulate the transcytotic potential of brain endothelial cells, on the transcytosis of prion-coated particles, will be investigated. In addition, as astrocytes may direct transferrin-coated poly-(lactic-co-glycolic acid) nanoparticles into distinct endocytotic pathways in endothelial cells,[34] it will be of interest to evaluate the effects of such environmental factors on the processing and transcytosis of prion-coated nanoparticles by the endothelial cells. This will provide detailed insight into the mechanism of PrPB transcytosis by hCMEC/D3 cells, clarifying the potential of prion-coated nanoparticles for drug delivery into the brain.

MATERIALS AND METHODS

Nanoparticles. A 50 mg/ml water suspension of 500-nm silica matrix magnetic core/green fluorescence (SiMAG/G) nanoparticles, functionalized either with hydroxyl, *i.e.* SiMAG/G-Hydroxyl (noncoated particles) or PEI, *i.e.* SiMAG/G-PEI (PEI-coated particles) were purchased from Chemicell (Berlin, Germany). Prion-coated nanoparticles were prepared by covalently coupling SiMAG/G-Hydroxyl with human prion protein (23–230), obtained from Allprion (Schlieren, Switzerland), at aseptic conditions according to manufacturer's protocol. Briefly, 10 mg SiMAG/G-Hydroxyl nanoparticles were washed once with 0.2 mol/l borate buffer (pH 8.5) using a magnetic separator and resuspended in 0.25 ml

borate buffer. 0.1 ml of 5 mol/l CNBr in acetonitrile (Sigma Aldrich, St Louis, MO) was added to activate the hydroxy-terminal groups of the SiMAG/G-Hydroxyl nanoparticles. The reaction mixture was kept for 10 minutes in ice-cold water. After washing twice with phosphate-buffered saline (pH 7.4), using a magnetic separator, the nanoparticles were resuspended in 0.25 ml phosphate-buffered saline, and 50 µg prion protein, dissolved in water, was added to the suspension. The coupling reaction was performed for 2 hours at room temperature. The freshly prepared prion-coated nanoparticles were washed three times with phosphate-buffered saline and stored in phosphate-buffered saline (0.1% bovine serum albumin). Each prion-coated nanoparticle contained ~0.83 nmol prion molecules, as determined in a 50 µg/ml particle suspension using a standard bicinchonic acid assay. The stability of the prion-coated nanoparticles was verified before use by measuring the release of prion protein at 280 nm using a NanoDrop ND-1000 spectrophotometer (NanoDrop Technologies, Wilmington, DE) which was typically negligible. Prion coating was also qualitatively confirmed by light microscopical evaluation of particle coalescence triggered by the addition of 20 µg/µl SAF32 to 10 µg/ml particles suspension, whereas antibodies against nonrelevant CD26 did not trigger particle coalescence (data not shown).

The size (hydrodynamic diameter) of the nanoparticles was measured in water using a Malvern Zetasizer nano-S (Malvern Instruments, Worchestershire, UK). Noncoated nanoparticles: 490.55 ± 0.21 nm, prion-coated nanoparticles: 738.25 ± 6.15 nm, PEI-coated nanoparticles: 539.65 ± 8.84 nm. The ζ potential was determined in water using a NICOMP 380 ZLS particle sizer (Particle Sizing Systems, Santa Barbara, CA). Noncoated particles: $Z = -26.33$ mV; prion-coated particles: $Z = -27.16$ mV; PEI-coated particles $Z = +27.95$ mV.

hCMEC/D3 cell culture. Human cerebral microvessel endothelial hCMEC/D3 cells[35] were maintained in 25 cm^2 flasks precoated with 100 µg/ml rat tail collagen type-I (BD Biosciences, Franklin Lakes, NJ) in endothelial basal medium-2 (EBM-2; Lonza Group, Basel, Switzerland), supplemented with EGM-2-MV bullet kit (Lonza) containing vascular endothelial growth factor, R^3-insulin-like growth factor-1, human epidermal growth factor, human fibroblast growth factor-basic, hydrocortisone, and 2.5% fetal bovine serum and 100 µg/ml penicillin/streptomycin. For differentiation of the cells EBM-2 basal medium was supplemented with 1 µmol/l dexamethasone (Sigma Aldrich) and 1 ng/ml bFGF (Invitrogen, Carlsbad, CA). Cells were maintained at 37 °C under an atmosphere of 5% CO_2.

Internalization of nanoparticles. A volume of 2×10^5 hCMEC/D3 cells were seeded onto glass coverslips, precoated with 100 µg/ml collagen type-I, and grown to confluency. These cells developed polarity, as evidenced by the polarized distribution of the abluminal (basolateral) plasma membrane protein platelet endothelial cell adhesion molecule, the tight junction–associated protein ZO-1 and the luminal (apical) plasma membrane protein multidrug resistance protein-1, which is dependent on the presence of functional tight junctions (**Supplementary Figure S1**). Cells were washed with EBM-2 and incubated in EBM-2 at 37 °C for 30 minutes. When indicated, inhibitors of endocytotic pathways [chloropromazine (5 µg/ml; Sigma Aldrich), filipin III (1 µg/ml; Sigma Aldrich), okadaic acid (150 nmol/l; Calbiochem, Gibbstown, NJ), dimethylamiloride (40 µmol/l; Sigma Aldrich), genistein (30 µg/ml; Sigma Aldrich)] were added during this step to preincubate the cells. Cells were then incubated with noncoated, PEI-coated or prion-coated nanoparticles, diluted in EBM-2 to a final concentration of 10 µg/ml, at 4 °C for 30 minutes (pulse-chase experiments), followed by a subsequent incubation at 37 °C for the indicated time intervals. Alternatively, cells were incubated with the nanoparticles directly at 37 °C for the indicated time intervals. When cells had been pretreated with inhibitors, these were kept present in all subsequent incubation steps. After extensive washing with ice-cold Hank's buffered salt solution to remove surface-bound nanoparticles, the cells were fixed with 2.4% paraformaldehyde (100 mmol/l sodium cacodylate, 100 mmol/l sucrose) and processed for immunofluorescence microscopy. The efficiency of the washing procedure was determined by performing the incubation with particles at 4 °C, which prevents their internalization. In this case, no cell-associated nanoparticles were detected.

Immunofluorescent labeling and image analysis. Fixed cells were permeabilized with 0.2% Triton X-100 at room temperature for 2 minutes. Caveolin-1 and clathrin immunolabeling was performed after methanol fixation for 5 minutes at −20 °C. Rabbit polyclonal anti-caveolin and mouse monoclonal directed against rat clathrin heavy chain were from BD Biosciences Pharmingen (Franklin Lakes, NJ), rabbit polyclonal anti-EEA-1 and rabbit polyclonal anti-Rab11a were from Abcam (Cambridge, MA) and Zymed Labs (San Francisco, CA), respectively, and mouse anti-rabankyrin-5 was a kind gift from Marino Zerial (Max Planck Institute of Cell Biology and Genetics, Dresden, Germany). Double labeling was performed by sequential incubation of the primary antibodies. Immunostaining with mouse monoclonal anti-LAMP1 H4A3 (Developmental Hybridoma Bank, University of Iowa) was performed after nanoparticles had been incubated with cells for 18 hours. In parallel, cells were incubated with Lysotracker Red DND-99 (Invitrogen) for 45 minutes, to visualize acidic compartments. The coverslips were mounted onto microscopic slides with Faramount aqueous mounting medium (Dako, Glostrup, Denmark). Images were acquired by confocal microscopy [Leica TCS SP-2 (Accusto-optical beam splitter)]. Although the nanoparticles were labeled by the supplier with a fluorescent dye (excitation 502 nm, emission 525 nm), we were unable to detect any fluorescence. Therefore, all the particles were detected by their reflection signal, obtained by excitation at 514 nm and collecting emission at the same wave length. Further image processing was with ImageJ software (National Institutes of Health, http://rsb.info.nih.gov/ij). After background correction, the colocalization analysis was performed according to the auto-thresholding method described in ref. 36. The colocalization data are presented as number of colocalizing pixels, between particles and the protein of interest, divided by the total number of particles pixels, and expressed as percentage. The experiment was performed at least two times in duplicate. From each sample at least five random fields were analyzed.

Electron microscopy. hCMEC/D3 cells were grown in 12-wells plates, precoated with collagen type-I. To the confluent monolayer, 10 µg/ml nanoparticles were added and incubated for 90 minutes. Subsequently, cells were washed with Hank's buffered salt solution and fixed in 2% paraformaldehyde plus 0.2% glutaraldehyde buffered with 100 mmol/l sodium cacodylate for 2 hours on ice. Samples were incubated with rabbit anti-caveolin-1 and mouse anti-clathrin heavy chain for 90 minutes at room temperature and with secondary antibodies, conjugated with 15- and 5-nm gold, overnight at 4 °C. Postfixation with 2% osmium tetroxide was for 30 minutes at 4 °C. Gradual dehydration was performed with increasing ethanol concentrations from 30 to 100%. The samples were embedded in EPON, and ultrathin sections were made and contrasted with uranyl acetate and lead citrate, according to routine procedures. Samples were examined with a Philips CM 100 electron microscope operated at 80 kV.

Transcytosis assay. A volume of 2×10^5 cells/cm^2 were seeded onto Transwell filters with a pore size of 3 µm (Corning, Corning, NY), and coated with collagen type-I. Media were changed three times a week and the transepithelial electrical resistance value was measured using a Millicell-ERS (Millipore, Billerica, MA). When hCMEC/D3 monolayers reached a transepithelial electrical resistance value of ~50 Ω/cm^2 (after 14–15 days), the experiments were performed. Nanoparticles (10 µg/ml), diluted in EBM-2 media, were added to the apical compartment and incubated for 18 hours at 37 °C. The media in the apical and basal compartment were collected and the filter membrane was cut from the support and soaked in water. 1.5 ml of 65% nitric acid (Acros Organics, Liège Area, Belgium) was added to the samples overnight to oxidize the iron.

The volume of the samples was adjusted to 5 ml with ultra pure water. The total amount of iron in the three compartments, *i.e.* apical, basal and the filter with cells, was quantified using inductively coupled plasma resonance mass spectrometry.

SUPPLEMENTARY MATERIAL

Figure S1. Polarized distribution of PECAM, ZO-1 and MRP-1 in hCMEC/D3 cells.

Figure S2. PrPBs are found in vesicles positive for both caveolin-1 and clathrin.

Table S1. The effect of metabolic inhibitors of endocytosis on the internalization of reference substances.

ACKNOWLEDGMENTS

We thank M. Zerial for generously providing the antibody against rabankyrin-5. We thank S. van IJzendoorn for critically reading the manuscript. This work was performed within the framework of the Dutch Top Institute Pharma project T5-105.

REFERENCES

1. Wolf, AA, Jobling, MG, Wimer-Mackin, S, Ferguson-Maltzman, M, Madara, JL, Holmes, RK *et al.* (1998). Ganglioside structure dictates signal transduction by cholera toxin and association with caveolae-like membrane domains in polarized epithelia. *J Cell Biol* **141**: 917–927.
2. Tuma, PL and Hubbard, AL (2003). Transcytosis: crossing cellular barriers. *Physiol Rev* **83**: 871–932.
3. Muro, S, Koval, M and Muzykantov, V (2004). Endothelial endocytic pathways: gates for vascular drug delivery. *Curr Vasc Pharmacol* **2**: 281–299.
4. Norkin, LC (2001). Caveolae in the uptake and targeting of infectious agents and secreted toxins. *Adv Drug Deliv Rev* **49**: 301–315.
5. Predescu, SA, Predescu, DN and Malik, AB (2007). Molecular determinants of endothelial transcytosis and their role in endothelial permeability. *Am J Physiol Lung Cell Mol Physiol* **293**: L823–L842.
6. Triguero, D, Buciak, JB, Yang, J and Pardridge, WM (1989). Blood-brain barrier transport of cationized immunoglobulin G: enhanced delivery compared to native protein. *Proc Natl Acad Sci USA* **86**: 4761–4765.
7. Kumagai, AK, Eisenberg, JB and Pardridge, WM (1987). Absorptive-mediated endocytosis of cationized albumin and a β-endorphin-cationized albumin chimeric peptide by isolated brain capillaries. Model system of blood-brain barrier transport. *J Biol Chem* **262**: 15214–15219.
8. Candela, P, Gosselet, F, Miller, F, Buee-Scherrer, V, Torpier, G, Cecchelli, R *et al.* (2008). Physiological pathway for low-density lipoproteins across the blood-brain barrier: transcytosis through brain capillary endothelial cells *in vitro*. *Endothelium* **15**: 254–264.
9. Fishman, JB, Rubin, JB, Handrahan, JV, Connor, JR and Fine, RE (1987). Receptor-mediated transcytosis of transferrin across the blood-brain barrier. *J Neurosci Res* **18**: 299–304.
10. Descamps, L, Dehouck, MP, Torpier, G and Cecchelli, R (1996). Receptor-mediated transcytosis of transferrin through blood-brain barrier endothelial cells. *Am J Physiol* **270**: H1149–H1158.
11. Zensi, A, Begley, D, Pontikis, C, Legros, C, Mihoreanu, L, Wagner, S *et al.* (2009). Albumin nanoparticles targeted with Apo E enter the CNS by transcytosis and are delivered to neurones. *J Control Release* **137**: 78–86.
12. Pardridge, WM, Buciak, JL and Friden, PM (1991). Selective transport of an anti-transferrin receptor antibody through the blood-brain barrier *in vivo*. *J Pharmacol Exp Ther* **259**: 66–70.
13. Fukuta, M, Okada, H, Iinuma, S, Yanai, S and Toguchi, H (1994). Insulin fragments as a carrier for peptide delivery across the blood-brain barrier. *Pharm Res* **11**: 1681–1688.
14. Rejman, J, Oberle, V, Zuhorn, IS and Hoekstra, D (2004). Size-dependent internalization of particles via the pathways of clathrin- and caveolae-mediated endocytosis. *Biochem J* **377**: 159–169.
15. Viegas, P, Chaverot, N, Enslen, H, Perrière, N, Couraud, PO and Cazaubon, S (2006). Junctional expression of the prion protein PrPC by brain endothelial cells: a role in trans-endothelial migration of human monocytes. *J Cell Sci* **119**: 4634–4643.
16. Banks, WA, Robinson, SM, Diaz-Espinoza, R, Urayama, A and Soto, C (2009). Transport of prion protein across the blood-brain barrier. *Exp Neurol* **218**: 162–167.
17. Roth, TF and Porter, KR (1964). Yolk protein uptake in the oocyte of the mosquito *Aedes aegypti*. I. *J Cell Biol* **20**: 313–332.
18. Tebar, F, Sorkina, T, Sorkin, A, Ericsson, M and Kirchhausen, T (1996). Eps15 is a component of clathrin-coated pits and vesicles and is located at the rim of coated pits. *J Biol Chem* **271**: 28727–28730.
19. Doherty, GJ and McMahon, HT (2009). Mechanisms of endocytosis. *Annu Rev Biochem* **78**: 857–902.
20. Schnitzer, JE, Oh, P, Pinney, E and Allard, J (1994). Filipin-sensitive caveolae-mediated transport in endothelium: reduced transcytosis, scavenger endocytosis, and capillary permeability of select macromolecules. *J Cell Biol* **127**: 1217–1232.
21. Parton, RG, Joggerst, B and Simons, K (1994). Regulated internalization of caveolae. *J Cell Biol* **127**: 1199–1215.
22. Aoki, T, Nomura, R and Fujimoto, T (1999). Tyrosine phosphorylation of caveolin-1 in the endothelium. *Exp Cell Res* **253**: 629–636.
23. Orlandi, PA and Fishman, PH (1998). Filipin-dependent inhibition of cholera toxin: evidence for toxin internalization and activation through caveolae-like domains. *J Cell Biol* **141**: 905–915.
24. Olusanya, O, Andrews, PD, Swedlow, JR and Smythe, E (2001). Phosphorylation of threonine 156 of the mu2 subunit of the AP2 complex is essential for endocytosis *in vitro* and *in vivo*. *Curr Biol* **11**: 896–900.
25. Shurety, W, Stewart, NL and Stow, JL (1998). Fluid-phase markers in the basolateral endocytic pathway accumulate in response to the actin assembly-promoting drug Jasplakinolide. *Mol Biol Cell* **9**: 957–975.
26. Liu, NQ, Lossinsky, AS, Popik, W, Li, X, Gujuluva, C, Kriederman, B *et al.* (2002). Human immunodeficiency virus type 1 enters brain microvascular endothelia by macropinocytosis dependent on lipid rafts and the mitogen-activated protein kinase signaling pathway. *J Virol* **76**: 6689–6700.
27. Schnatwinkel, C, Christoforidis, S, Lindsay, MR, Uttenweiler-Joseph, S, Wilm, M, Parton, RG *et al.* (2004). The Rab5 effector Rabankyrin-5 regulates and coordinates different endocytic mechanisms. *PLoS Biol* **2**: E261.
28. Marella, M, Lehmann, S, Grassi, J and Chabry, J (2002). Filipin prevents pathological prion protein accumulation by reducing endocytosis and inducing cellular PrP release. *J Biol Chem* **277**: 25457–25464.
29. Rajendran, L, Knölker, HJ and Simons, K (2010). Subcellular targeting strategies for drug design and delivery. *Nat Rev Drug Discov* **9**: 29–42.
30. Brandner, S, Klein, MA and Aguzzi, A (1999). A crucial role for B cells in neuroinvasive scrapie. *Transfus Clin Biol* **6**: 17–23.
31. Lasmézas, CI, Cesbron, JY, Deslys, JP, Demaimay, R, Adjou, KT, Rioux, R *et al.* (1996). Immune system-dependent and -independent replication of the scrapie agent. *J Virol* **70**: 1292–1295.
32. Banks, WA, Niehoff, ML, Adessi, C and Soto, C (2004). Passage of murine scrapie prion protein across the mouse vascular blood-brain barrier. *Biochem Biophys Res Commun* **318**: 125–130.
33. Tang, Y, Han, T, Everts, M, Zhu, ZB, Gillespie, GY, Curiel, DT *et al.* (2007). Directing adenovirus across the blood-brain barrier *via* melanotransferrin (P97) transcytosis pathway in an *in vitro* model. *Gene Ther* **14**: 523–532.
34. Chang, J, Jallouli, Y, Kroubi, M, Yuan, XB, Feng, W, Kang, CS *et al.* (2009). Characterization of endocytosis of transferrin-coated PLGA nanoparticles by the blood-brain barrier. *Int J Pharm* **379**: 285–292.
35. Weksler, BB, Subileau, EA, Perrière, N, Charneau, P, Holloway, K, Leveque, M *et al.* (2005). Blood-brain barrier-specific properties of a human adult brain endothelial cell line. *FASEB J* **19**: 1872–1874.
36. Costes, SV, Daelemans, D, Cho, EH, Dobbin, Z, Pavlakis, G and Lockett, S (2004). Automatic and quantitative measurement of protein-protein colocalization in live cells. *Biophys J* **86**: 3993–4003.